J. Eng. Sci., King Saud Univ., Vol. **11** (2), 179-200 (1985)

Rain Measurements for MM-Wave Propagation: A Review

Mohamed Hassan, Adel Ali and Mohammed Alhaider

Electrical Engineering Department, College of Engineering, King Saud University, Riyadh, Saudi Arabia

This paper is a review of rain parameters, and their measurements, pertinent to electromagnetic wave propagation at super-high frequency (SHF) and extremely-high frequency (EHF) parts of the spectrum. The rain-rate parameter is first presented along with the major experimental studies on rain-rate statistics. Other rain parameters, including drop-fall speed, drop-shape, drop-size distribution and canting angle, are also dealt with. Direct and indirect methods of measuring rain parameters are then addressed, together with a description of the instruments used. Direct rain measurements performed using rain-rate gauges, distrometers or rain analysers are outlined with a comparison of various types of rain-rate gauge. Indirect rain measurements using weather radars and radiometers are also given. The advantages of using radar for measuring rain parameters are explained and compared with direct rain measurements. The other type of indirect measurement, namely using radiometers, is described in detail, with a summary of types of radiometer. A mention of areas which need further study is also given. Six tables are provided to summarize main experiments and to compare various instruments.

1. Introduction

Rainfall is one of the important factors affecting the propagation of the waves in the millimetre waveband. Rain data have been collected over many decades by local hydrological departments using standard instruments with long integration periods. These data only give a general idea about precipitation in such a region and are not in a form applicable for predicting radio-link reliability. Therefore, the study of rainfall characteristics inherent with radio-wave propagation at some location is of great value.

The following measurements are useful for studying the effects of rainfall rate on millimetre wave links:

(i) the annual probability distribution of point rain rates, i.e. percentage of year for which rain rate is exceeded.

(ii) average number of occasions per year when specified rain rate is continuously exceeded for certain duration, or has return periods exceeding some value.

Other rain parameters such as drop size, drop shape and canting angle have profound effects, as well, on the propagation of waves at extremely-high frequencies.

As rainfall affects the propagation of the millimetric wave, rainfall is also affected by several other factors, such as wind velocity and temperature [1]. It is usually assumed that drops fall at their terminal velocities in still-air. However, during a turbulence condition, a vertical wind velocity component is present. In this case, raindrop density in the microwave beam does not change but the rain rate measured at the ground is altered considerably, and causes uncertainty in the correlation of attenuation and rain-rate measurements. The complex dielectric constant of rainfall water is changed with temperature, thus altering the values of the attenuation coefficient. However, this effect is not very significant.

Two different approaches to the estimation of rain attenuation are possible, one based solely on the use of a large number of attenuation variations at different frequencies, locations and path geometries, and the other based on the synthesis of attenuation values from meteorological data. The latter is most promising at the current time because a considerably larger data base is available for use in estimating the distribution functions required for modelling path attenuation [2].

This paper surveys the recent experiments aimed at measuring rain parameters pertinent to wave propagation. Various direct-measuring and indirect-measuring instruments are described as well, together with references to main experiments where such instruments were used. The paper is concluded by an outline of some areas where further work is still needed. It is hoped that the paper will be of particular interest to communication engineers and meteorologists planning a study of wave propagation at extremely-high frequency (EHF).

2. Rain-Rate Parameter

Attenuation statistics, i.e. the percentage of time of attenuating radio waves, are necessary for millimetric-wave radio-link planning. These can be derived from statistics of rainfall rates (or rainfall intensity, i.e. the quantity of water falling per unit time). Rainfall can be classified according to its intensity in mm/hr as given in Table 1.

Table 1. Types of Rain

Rain Type	Light Drizzle	Drizzle	Light Rain	Medium Heavy Rain	Heavy Rain	Intense Rain	Tropical Downpour
Rainfall Intensity mm/hr	0.25	1.25	2.5	12.5	25	50	100–150

Rain rates are usually measured at a point by means of a rain gauge, preferably having an integration time of the order of 1 min. or less [3]. However, the point rain rate may not represent the rain rate along the path, unless rainfall is considered to be uniform. In a rain storm, the entire radio path is not generally in the rain area. Rain cells possibly cover from about one kilometre to several kilometres of the path during the rainfall period. Meteorological experience shows that rain of short duration tends to be restricted to a relatively small geographical area. This fact is expressed by the so-called area-depth curves [4] shown in Fig. 1. It also shows that the average rain-cell size decreases as the rainfall-rate increases [5], as shown in Fig. 2.

When the cell diameter is smaller than the path length, the actual attenuation would be less than that derived from a point rain rate. For better estimation of rain attenuation on a link, the average rain rate along the path—called the *line rate*—is needed. This can be obtained by operating a sufficient number of rapid-response gauges, recording the variations of point rain rates along the path, which is inconvenient and impractical. An alternative method is to obtain statistical relationships between line and point rain rates.

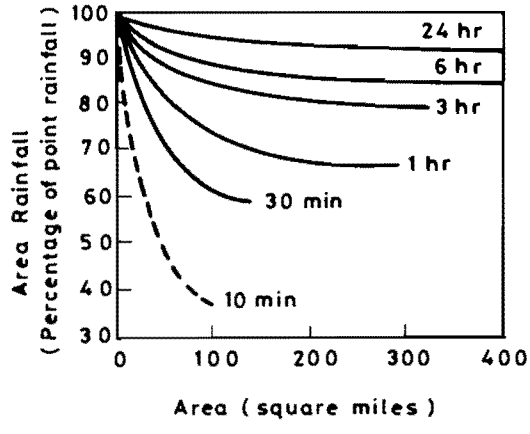

Fig. 1: Typical Area–Depth Rainfall Curves.

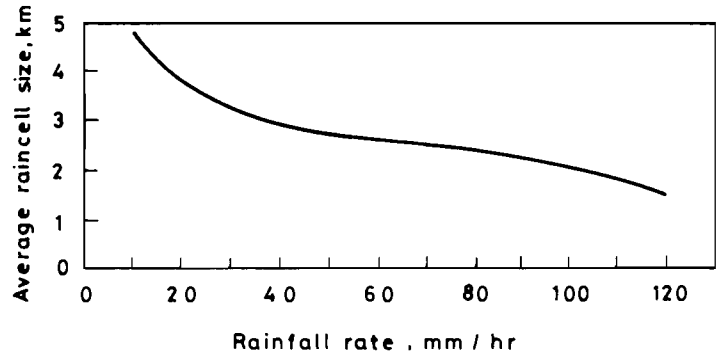

Fig. 2: Average Rain-Cell Size vs Rain Rate.

Harden *et al.* [6] gave a relationship between point and line rates for distances up to 8 km and for different percentages of time. From the point rainfall rate data collected over a 20-year period for different locations in England [7], they also obtained the probability distributions of point rain rates. These are modified with temporal and spatial factors—derived from both long-term and short-term rainfall records—in order to obtain the probability distributions of line rates. This latter was then used to find the attenuation statistics.

Harden *et al.* [6] and Norbury *et al.* [8] showed that measured probability distributions usually vary from year to year. They also tabulated factors for converting these distributions of rain rate from one integration to another. They derived models for the intensity-time and intensity-distance profiles of intense rain events at Slough, England.

Weibel and Dressel [4] set up an experimental link and found the cumulative probability distribution for rainfall rates at Washington D.C., and expected it to represent the rainfall characteristics in most areas at middle latitudes.

Using the data collected during four years of continuous measurements of surface point rain rates in Clarksburg, Maryland, Kumar [9] obtained the probability distribution of surface-point rates for the first year, the second year, the last two years, and the entire measurement period. He found no significant difference in the total accumulation of rain for each year.

Harman [10] compared the accumulations measured over several years in Rosman, N.C., with those obtained in the years 1970 and 1971, and found it to be typical. He also found that short-term rain-rate distributions can vary from time to time in a particular year and even for the same time periods in different years. Rain-rate distributions for 1970 and 1971 were similar, and hence considered to represent the typical rain-rate distributions for the Rosman area.

In the experiment carried out by Mogensen and Stephansen [11] on a 44.7 km radio link operating in the frequency range 13.5–15.0 GHz in Copenhagen, Denmark, seven rapid-response drop-counting rain gauges were used. The gauges were placed in the vicinity of the path. They found that the average probability distribution of the seven observed rain rates along the path for each of these integration times (0.5, 5, 50 min.) was statistically more stable compared with the individual distributions.

Some of the above experiments are summarized in Table 2.

Table 2. Experiments on Rain Statistics

Authors	Place	Period	Main Results
Harman [10]	Rosman, N.C.	1970–1971	Yearly accumulation is about the same. Yearly rain-rate distribution is about the same. Short-term rain-rate distribution can vary from time to time in a particular year.
Kumar [9]	Clarksburg, Maryland	July 76–Sept. 80	Yearly accumulation is about the same. Probability distributions of surface-point rates for 1st year, 2nd year, last two years, and the four years are obtained.
Harden *et al.* [7]	Different locations in England	20 years	Modification of probability distributions of point rain rates to probability distributions of line rates through temporal and spatial factors.
Harden *et al.* [6]	Slough, England	1970–76	Factors for converging rain-rate probability distributions from one gauge integration time to another. Statistical models of intense rain events in U.K.
Mogensen *et al.* [11]	Copenhagen, Denmark	May to Oct. 1975–June to Sept. 1977	Average probability distribution is more statistically stable than individual distributions.

3. Other Rain Parameters

In order to calculate rain-induced attenuation, the *drop-size distribution* and *drop-fall speed* must be found. Also, rain rate can be calculated if both parameters are known [12, 13]. *Drop shape* is the main cause of differential attenuation on links using orthogonal linear polarizations. Frequency re-use in orthogonal polarization is limited by cross-polarization caused mainly by *drop canting*.

3.1. *Drop-Fall Speed*

Gunn and Kinzer [14] determined experimentally the fall speed of raindrops. Fall speed increases as the drop size increases [15]. It ranges from 206 to 914 cm/sec for drop diameters of 0.5 to 6.5 mm respectively.

3.2. *Drop Canting*

The canting angle is defined [16] as the angle between the major axis of the image of an oblate raindrop projected on a plane normal to the direction of propagation with respect to the horizontal. Raindrop canting is mainly caused by the vertical wind gradient, i.e. the wind speed as a function of height [17]. Actual canting-angle measurements are very difficult to carry out.

3.3. *Drop Shape*

At EHF, rain-induced attenuation is the most important factor on the mmw propagation and may be derived for spherical drops. However, on links using orthogonal linear polarizations, differential attenuation has been measured. This is due to the fact that raindrops change form during their fall. The mean shape of the drops is oblate instead of spherical [18]. Pruppacher and Pitter [19] showed that the oblate spherical shapes are dominant except for the very largest drops. Raindrop deformation increases as the drop size increases [15]. The cross-polarization (the amount of cross-coupling between orthogonal polarizations) effects during rain may be explained by assuming that the drops not only have a shape other than spherical but also a mean canting angle different from zero [51].

3.4. *Drop-Size Distribution*

For the estimation of attenuation along a path, the specific attenuation at each point along the path is required. The specific attenuation is theoretically related to the instantaneous rain rate using measured or modelled raindrop-size distribution.

Laws *et al.* [20] derived a raindrop-size distribution from ground-based pellet measurements, and put it in a tabulated form, to become one of the most commonly used distributions. Other drop-size distributions were proposed by Marshall and Palmer [21] and by Joss *et al.* [22]. Joss *et al.* found that large variations in these distributions occur not only for different types of rain but also during one shower. Average distributions were found to be applicable for three types of rain (drizzle, widespread and thunderstorm). The Marshall–Palmer distribution and all three Joss *et al.* distributions are of the negative-exponential type expressed by [23]

$$N = N_0 \, e^{-\lambda D}, \qquad \lambda = qR^{-0.21}$$

where

N = number of drops per unit volume per unit diameter

D = drop diameter (mm)

R = rainfall rate (mm/hr)

$N_0 (\mathrm{m}^{-3}\,\mathrm{mm}^{-1})$ and $q\ (\mathrm{mm}^{-1})$ are constants

depend on the type of rain as follows:

Drop-size distribution	N_0	q
Marshall-Palmer	8000	4.1
Joss *et al*: drizzle	30,000	5.7
Joss *et al* widespread	7000	4.1
Joss *et al* thunderstorm	1400	3.0

Good results were obtained using these modelled distributions, although the Laws-Parsons raindrop size seems to provide more accurate results [5]. However, it is always preferable to base rain attenuation calculation on the actually measured drop-size distribution, as the latter varies even from the same location. This raindrop size distribution is usually measured by counting the number of droplets for each diameter by measuring the diameter itself and any of the rated physical quantities such as the cross-section, the volume, the mass, the momentum, the electric charge, the acoustic strength, or the falling velocity of the droplet.

Keizer *et al.* [13, 23] catalogued the measured drops into 20 classes of size, then the number of drops per unit volume for each of these classes was calculated. Sander [12] classified the measured raindrops into 16 sizes, and also showed that simultaneous measurements of attenuation at two frequencies permits the evaluation of drop-size distribution. Furuhama [24] used two methods:

(i) a direct method by measuring the raindrop-size distribution with a distrometer;

(ii) an indirect method by measuring the attenuation, then deriving the path-averaged drop-size distribution.

4. Rain Measurements and Instrumentations

4.1. *Direct-Rain Measurements*

4.1.1. *Rain-rate Gauges.* The rain-rate gauge is a device designed to measure rainfall rate at a point. Many new rain gauges with improved designs are available and increasing every year. The trend now is towards devices of small size bringing about fewer environmental disturbances.

Rainfall is usually averaged over the integration time of the rain gauge. This time must be short enough not to miss any deep fade, and such that the point rain-rate distribution best approximates the path-averaged rain-rate distribution. It is found to be [25]:

$$T = 1.05 \frac{\sqrt{\lambda L}}{\pi} \ln 32 \frac{L}{\lambda} \tag{1}$$

It is a function of path length L and wavelength λ. The most intense rainfall rate must be measured by rapid-response gauges, i.e. of low integration time, specially constructed for radiometeorological purposes. A comparison of three of them is given in Table 3.

Using a fast-integrating rain gauge, Bodtmann and Ruthroff [25] measured the rain-rate distributions as a function of integration time, T, in Holmdel, N.J., for the two years 1971-1972. They found that for many paths, a one-minute integration time is adequate enough for rain rates as high as 120 mm/hr. They confirmed that a short integration time for the rain-rate measurement is required to approximate the path-averaged rain rate or the attenuation by a single-point rain rate. They also concluded that the use of rain gauges with slow response underestimates point rainfall intensity.

Table 3. Comparison of Three Rain Gauges

Fast-Integrating Rain Gauge [25]	Capacitor Depth Gauge [3]	Tipping-Bucket Rain Gauge [50]
Measures rain rates in accordance with the requirements of the theory for fast integration time of rain rate.	Measures rain rates in accordance with the definition $\frac{1}{T_0}\int_{t}^{t+T_0} R_D(u, v; t)\hat{r}\,dt$ This is the rain rate at point (u, v) averaging over time T_0. $\hat{r}$ is a unit vector.	Measures rain rate by counting raindrops of constant volume during 10 sec intervals.
Basic elements Big funnel 16 in. diameter, small rotating funnel, four glass tubes, two metallic plates attached to the outer surface of each tube.	*Basic elements* Funnel, cylindrical capacitor, shutter for draining the capacitor, a number of depth gauges, a rotating shield.	*Basic elements* Collecting funnel, totalizer, tipping bucket, drop sensor between funnel and tipping bucket.
Operation 1) The rain is collected in the big funnel in 1.5 sec interval. 2) The small rotating funnel directs the water to one of the four glass tubes, then rotates to the next tube. 3) Water volume is measured by measuring the capacitance between the two metallic plates. 4) After measurement, tube is emptied and is ready to be used again.	*Operation* 1) Funnel exposed to the rain for a specified time T and then covered. 2) This rain drains into the cylindrical capacitor and forms a column of water. 3) The capacitance is measured. The greater the height of the water column, the greater the capacitance. 4) When a depth gauge terminates the collection of rain, the shield rotates, covers it and exposes the next depth gauge.	*Operation* 1) The tipping bucket and drop-counting unit are used to digitize the rainfall intensities. 2) The drop sensor gives the exact time information of the start of rainfall. 3) An electric impulse is generated with each tip of the bucket and is transmitted via a two-conductor cable to a receiving mechanism. 4) The water is discharged automatically from the bottom.
Integration time Multiples of 1.5 sec.	*Integration time* It can be determined precisely by careful operation of the shield.	*Integration time* (i) It is 10 sec. (ii) For longer integration periods, rates over successive 10 sec intervals are averaged together.

Hata *et al.* [26] used three rain gauges to measure the rain rate of precipitation on a 1.08 km link in Nagoya city, Japan, operating at 23 and 40 GHz. Two rain gauges, one of the drop-counting type with one-minute integration time and the other of the tipping-bucket type, were used at both sites. A third rain gauge of the drop-counting type with 10-sec integration time was also used at the middle of the link's path. They concluded that heavy-rain statistics obeyed Poisson's distribution, and that the best-fit rain gauge integration time was about half a minute for the 23 GHz, 1.08 km link.

Norbury *et al.* [6, 8] set up several rapid response rain gauges [27] measuring rain fall rates over 10 sec intervals at Slough. Measurements were recorded when rain rate exceeded 5 mm/hr. During the period from December 1969 to April 1971, four gauges were situated 5 m apart and 50 cm above ground level. From April 1971 to November 1971 three of them were placed 4 m above ground level and spaced 45 m along the radio link. Measurements [6] were also taken at Mendlesham from gauges spaced about 400 m along the 7.5 km path. They reported cumulative distributions of rain rate for the two above-mentioned periods, the durations of falls and the time intervals between them when exceeding specified intensities. They also showed [1] that the error of mean attenuation coefficient reduces as the number of gauges increases, and as the response time decreases.

4.1.2. *Distrometers.* The distrometer is an instrument used to obtain the drop-size distribution at a point along the radio path. The measured drop-size distribution, which is time dependent, can easily be transformed into rain intensities. Its theory is based upon an electrodynamical receptor which changes the impulse of a falling raindrop into an electric signal. A distrometer [23] performs the following functions:

(i) it measures the moments of drops falling on an electromagnetic sensor of $50 \times 50\ \text{cm}^2$ area;

(ii) it distinguishes between drops with a time spacing of about 1 m sec;

(iii) it can measure diameters between 0.3 and 5 mm.

The measured drops are catalogued into 20 classes of size with a resolution ΔD_i varying from 0.1 mm for small drops to 0.5 mm for large drops. The number of drops per unit volume (m^{-3}) is then calculated from

$$N(D_i)\Delta D_i = 10^4 \frac{N_i}{ST_s v(D_i)} \tag{2}$$

where,

N_i = number of drops with diameters between $D_i - 0.5\,\Delta D_i$ and $D_i + 0.5\,\Delta D_i$ (mm)

S = collecting area of the distrometer (cm^2)

T_s = time during which N_i drops strike the surface (sec)

$v(D_i)$ = fall velocity of a drop with diameter D_i (m/sec)

ΔD_i = resolution (mm).

In addition to the above-described distrometer, two other types were developed to overcome its poor response to small drops:

(i) one type measures the interruption to a light beam caused by falling raindrops [28];

(ii) another distrometer observes the shadow of particles on a large number of optical sensors. This is used for drop-shape observations as well [29].

Using distrometers, Joss *et al.* [30] confirmed that there is a large spatial and temporal variability in the raindrop parameters. Also, they found that for moderate and heavy rainfall, the attenuation calculated from the measured drop-size distribution and the measured attenuation are in good agreement. This was not the case for light rain. They also observed that ground-based distrometers 100 m apart are too close to give independent drop-size distributions.

Keizer *et al.* [13, 23] measured the raindrop-size distribution with a distrometer in order to calculate rain attenuation, which was found to be in agreement with measured data. The measured drops were catalogued into 20 classes of size, from 0.3 to 5.0 mm in diameter, then the number of drops per unit volume for each of these classes was calculated. They found the same results as those obtained by Joss *et al.* [30].

Furuhama [24] measured the raindrop-size distribution at the receiving site by the use of the distrometer. He also found the path-averaged drop-size distribution by measuring the attenuation on four links working on different frequencies. Both distributions were then compared. Diameters between 0.3 and 5.0 mm were covered by a distrometer whose collecting area was 50 cm^2.

4.1.3. *Rain Analyser.* This is another instrument for measuring the drop-size distribution, and hence the rainfall rate. It collects raindrops with a collecting area of about 100 cm^2. According to its size, each raindrop produces an electrostatic charge when falling through the first grid. On a second grid, the electrostatically-charged drops induce voltage pulses. Their amplitudes are measured and recorded under several drop-size classes, 0.4 mm in diameter and above. The rainfall rate can then be calculated from that measured drop-size distribution and the fall speed of the drops.

Using rain analysers, Sander [12] measured the raindrop size having diameters more than 0.7 mm with a collecting area of 25 cm^2. They were divided into 6 classes. Drop sizes in excess of 0.4 mm in diameter were measured as well with a collecting area of 100 cm^2 and classified into 16 classes of size. They found that at higher rain rates of rainfall, the drop-size distribution shifts to larger drops, hence giving higher attenuations.

4.2. *Indirect Rain Measurements*

4.2.1. *Weather Radars.* Radars are used to measure rainfall and attenuation in many experiments. They can indirectly measure drop size; however, the sensitivity is not adequate. Weather radars operate in the centimetre band and are used to determine the speed and direction of movement, and the location of rain cells within a large area around the station. They can also determine the horizontal and vertical cell structures. In the millimetre frequency band, they can be used to analyse and forecast the propagation conditions.

The main advantages of radars are as follows.

(i) Real-time (immediate) data can be collected in considerable detail.

(ii) They have a wide range for measuring rain rates (between 0.3 and 100 mm/hr).

(iii) They have a large coverage area (thousands of km^2) of rainfall rates, statistics, and the enormous sample size of attenuation events can be collected in a few days.

However, radars result in some errors, from which we state the following.

(i) Radars are not able to distinguish between different types of storm (rain, snow, sleet).

(ii) For a given rainfall rate, different reflectivity factors can be obtained.

(iii) Errors due to the fact that radar can only see a part of the precipitation occur. These errors increase as the range increases.

Table 4 summarizes a comparison between characteristics of both radars and rain gauges.

Two weather radars operating at 5.6 cm were installed [31] in La Dole and Albis, Switzerland, in 1977 and 1979 respectively. A complete volume scan, made by the radars every 10 min, contained the information of 19 antenna elevations up to a distance of 230 km and a height of 12 km. A computer was used to calculate a three-dimensional picture, giving a survey of all the relevant features of the current precipitation. Daily amounts of rain were found. Both radars measured on the average 20% of the precipitation recorded by the rain gauges.

Table 4. Comparison between Characteristics of Radars and Rain Gauges

Radars	Rain Gauges
1. Can measure between 0.3 and 100 mm/hr.	1. Can measure between 0.25 and 200 mm/hr and more.
2. Can cover several thousands of km^2.	2. Only rain rate at a point.
3. Can give rain measurement at the centre of a rain cell.	3. Rain cell may not pass over the gauge.
4. Accuracy of measuring rain rate at a single point is not as good as in a rain gauge.	4. Accuracy of measuring rain rate at a point by a good rain gauge is high.
5. Rainfall data collected over large area for a short time.	5. Rainfall data collected at a point for a long time.
6. Effects other than that of rain can be identified.	6. Measures only rain effects.
7. Must be used with a rain gauge for calibration but unchallenged when used over large area at heights well above ground level.	7. Essential for continuous calibration.

During the summer of 1973, Goldhirsh and Robinson [32] measured the rain reflectivity environment out to 140 km from the radar facility at Wallops Island, Va. These data, recorded on a digital tape, were injected into modelling procedures to obtain attenuation and path-diversity statistics at frequencies 13 and 18 GHz over variable path elevation and azimuth angles.

Between 1977 and 1980, Goldhirsh [33] used the SPANDAR-S-band radar at Wallops Island, Va, to collect rain data at 0.5° over the range 8 to 100 km. He also used a distrometer to measure the drop-size distribution and to derive the parameters A and B of the empirical relation:

$$R = AZ^B \tag{3}$$

where Z is the radar reflectivity factor. He determined 84 horizontal profiles of rain-rate structure, from which the cell-size statistics were developed.

Awaka *et al.* [34] conducted an experiment at 34.8 GHz in order to examine the effect of rain attenuation on the received power from rain scattering. Observations were made by the 5.33 GHz rain radar at Kashima, Japan, between June and October 1980. They found that a small cell with high rainfall rate caused a strong received power from rain scattering at 34.8 GHz.

Using the same 5.33 GHz radar, a radiometer and some meteorological instruments, Fujita *et al.* [35] determined the cumulative distribution of ground-rainfall rate over one year (1977–1978) at the Kashima earth station of the ETS-II satellite.

Hewitt and Norbury [36] recorded radar photographs, rain gauge measurements and microwave data to assist in extrapolating the results obtained from one area to other parts of the United Kingdom.

4.2.2. *Radiometers.* The radiometer is an instrument used to measure the attenuation due to absorption and/or scattering from atmospheric particles, e.g. rain, snow, cloud. It is often used to obtain attenuation statistics by estimating the attenuation from observed values of its antenna temperature. It can be used as an alternative to radar.

Radiometric measurements are usually carried out in conjunction with direct satellite radio-path attenuation measurements to verify correlation of fading and correlation of statistics of fading given by the two techniques [37].

Radiometers can also be used for monitoring weather patterns. From the cumulative distribution of attenuation measured using radiometers, one can construct the cumulative distribution of *apparent rain rate* corresponding to that attenuation statistics. The apparent rain rate is different from the path-averaged rain rate, and is expected to have a greater probability of occurrence than the point rain rate. This is because the apparent rain rate applies to an occurrence on a long path along the radiometer beam. The cell size can also be obtained from the absolute value of attenuation.

Modes of Operation

Radiometers can be operated in two modes [38–43]:

(i) the absorption mode, in which the radiometer is set with the antenna pointing toward the sun and moving with it slowly as the sun moves from east to west. The hour-angle motion for tracking the sun during any one day is provided by driving the reflector about its polar axis at a 24-h per revolution rate. The attenuation measurements in the absorption mode are taken with the sun as a source;

(ii) the emission mode, in which observations are taken with the parabolic antenna looking at the sky at different elevation angles.

Types of Radiometer

Radiometers are of several types [42–48]:

(i) the single feed conventional Dicke-type radiometer can be operated in a mode in which the sun is tracked continuously. It is a solar-tracker radiometer, and can measure values of attenuation up to about 10 dB;

(ii) the total power radiometer, whose dynamic range is also limited to 10 dB, measures attenuation derived from sky-emission data;

(iii) the nodding radiometer provides consecutive measurements of the sun and sky signals, and its dynamic range is 15 dB. The antenna beam nods on and off the sun with a maximum excursion of about 3° and a cycle time of 1 min.;

(iv) the fast-response dual-feed beam-switching radiometer has a dynamic range of 15 dB. It has two feeds defining the axes of two radio beams, one directed at the sun and the other at the sky about 3° away. In this way, a monitor of solar emission (or attenuated solar emission) with respect to that of adjacent sky (or rain) is obtained over a measuring range of 15 dB. This radiometer enables the difference between the sun and sky signals to be recorded directly. The beamwidth of the antennas is about 1°. Apart from the two feeds, the radiometer may be of a conventional Dicke-type with a ferrite switch alternately switching the signal from each beam into the receiver at a rate of 3 kHz.

Table 5 is a summary of the different types of radiometer along with their inherent merits and demerits.

Methods of Attenuation Calculation

The atmospheric attenuation can be derived in conjunction with radiometric measurements of emission from the sun, T_{sun}, and emission from the sky, T_{sky}.

T_{sun} = antenna temperature of the sun in the presence of attenuation + sky emission in presence of atmospheric absorption = $(1-a)T_s + T_{sky}$

where,

T_s = antenna temperature of the sun when no absorption occurred along the path

$T_{sky} = T_{at}$, for direction away from the sun

T_{at} = kinetic temperature of the atmosphere along the path, ≈ 275 K

a = instantaneous value of the fractional absorption along the path

Two methods can be used to derive the attenuation [37-39, 47-49]:

(i) the direct method, which compares the attenuated solar signal $k^*(1-a)T_s^*B$ with the unattenuated solar signal $k^*T_s^*B$, gives

$$\text{Attenuation (dB)} = 10\log_{10}\frac{kT_sB}{k(1-a)T_sB}$$

$$= 10\log_{10}\frac{1}{(1-a)} \qquad (4)$$

where k is Boltzmann's constant and B is the given bandwidth;

(ii) the indirect method, which only involves the measurement of the sky signal, T_{sky}, gives:

$$\text{Attenuation (dB)} = 10\log_{10}\frac{T_{at}}{T_{at}-T_{sky}} \qquad (5)$$

Table 5. Summary of Types of Radiometer

Technique	Mode of Operation	Elevation Angles	Radiometer Type	Merits	Demerits
Sky emission	Emission mode uses indirect method of attenuation calculation	Fixed angles of elevation	Total power radiometer	Continuous data. Measurements can be made at any angle either day or night very rapidly	Accuracy is questionable. Max dynamic range is 10 dB. Not convenient for above 15 GHz. Large errors due to assumption of T_{at} = 275 K
Sun emission	Absorption mode uses direct method of attenuation calculation	Solar-tracker	Single-feed conventional Dicke-type radiometer. Nodding radiometer. Fast-response dual-feed beam-switching radiometer	Direct measurement over large dynamic range. Measurements quite accurate under conditions of precipitation	Data not continuous. Daytime measurement only. Analysis is complicated

Radiometer Measurements

Several authors employed microwave radiometers for measurement of attenuation and absorption due to precipitation, and hence derived rain-rate statistics. Hogg *et al.* [16], in their experiment on rain attenuation on earth-space path at 16 and 30 GHz, measured during 1968 the cumulative attenuation distributions in New Jersey using the sun-tracker radiometer. From these measurements, they derived the cumulative apparent rain-rate distributions. It was concluded that the apparent rain-rate distribution is of higher occurrence than the point rain-rate distribution.

In New Delhi, Raina and Uppal [41] measured the rain-attenuation distribution by a microwave radiometer operating at 11 GHz for more than three years. They found that maximum attenuation was obtained during the monsoon period. The relation between the effective distance and the rain rate was obtained as well, where the effective distance is defined as the portion of the earth-space path that the wave travels under uniform rainfall.

In a path-diversity experiment carried out in New Jersey, U.S.A., Wilson *et al.* [49] used three radiometers operating at 16 GHz. The radiometers were located on a line extending from northwest at Sayreville—passing through Crawford Hill—and ending by Ashbury Park in the southeast, the distances being 11.2 km and 19.2 km respectively. The antennas were pointed at an azimuth of 226° and at an elevation of 32°. Their directions were appropriate for a domestic communication satellite in synchronous orbit. Recording was made only when a significant change in one of the three radiometers data value occurred. They gathered attenuation statistics to help them in designing a communication satellite system.

Davies conducted many experiments for over ten years at Slough, England, using solar-tracking radiometers, such as the 19 GHz conventional Dicke-type radiometer, and the 37 GHz and 71 GHz beam-switching radiometers [45, 46, 48]. In a trial for improving reliability on earth-space links, he carried out a diversity experiment using three 37 GHz radiometers. The first was located at Slough, the second at Winkfield 10.3 km southwest, and the third was put into operation at Hurley 18.5 km northwest of Slough. Least space diversity advantage was obtained when the sites were aligned approximately perpendicular to the direction of storm movement.

Some of the experiments described in Section 4 are summarized in Table 6.

5. Further Needed Measurements

1. To date, insufficient data on the spatial variation of rain are available to construct a creditable model for use in obtaining attenuation statistics from climatological data.
2. The effect of space diversity on overcoming deep fades caused by rain cells should be examined for different frequencies and rain climates.

Table 6. Experiments Using Different Instrumentations

Authors	Instruments	Main Results
Bodtmann *et al.* [25]	Fast-integrating rain gauge	1-min. integration time is accurate for rain-rate and attenuation measurements
Norbury *et al.* [1]	Rapid-response rain gauges	Attenuation coefficient error reduces as the number of gauges increases, and the response time decreases
Joss *et al.* [30]	Distrometers	Distrometers 100 m apart are too close to give independent drop-size distribution
Keizer *et al.* [13]	Distrometers	Attenuation calculated with measured drop-size distribution agrees well with attenuation measured
Sander [12]	Rain analyser	Drop-size distribution shifts to larger drops at higher rain rates
Hewitt *et al.* [36]	Radar	Extrapolation of results obtained from one area to other parts of U.K.
Goldhirsch [33]	Radar	Cell-size statistics were developed
Hogg *et al.* [16]	Radiometers	Apparent rain-rate distribution (using radiometer) is of higher occurrence than the point rain-rate distribution (using rain gauge)
Raina *et al.* [41]	Radiometers	Relation between effective distance and rain rate

3. The dependence of the point-rate distribution on rain-gauge integration time has to be established.
4. Long-term measurement of attenuation over existing links, followed by a comparison with nearby meteorological data, is needed in order to improve our understanding of data needed for link design.
5. Knowledge of raindrop canting angle distribution is very scarce and further study is required. Other rain anisotropies causing depolarization should be further examined, and a systematic method of obtaining such parameters as rain-size distribution and shapes using simple attenuation measurements are still lacking.

6. Conclusion

This paper has presented a tutorial on the rain parameters, and their measurements, pertinent to electromagnetic wave propagation at super-high frequency and extremely-high frequency. Various rain parameters are described as a main parameter, namely rain rate and other parameters which cause signal depolarization. Types of rain gauge, which measure rain parameters directly, are explained and compared. Indirect methods of measuring rain, which include radiometers and radars, are also discussed. In all cases, major experimental work is mentioned. Areas of further-needed measurements are emphasized.

References

1. **Norbury, J.R.** and **White, W.J.K.**, Correlation between measurements of rainfall rate and microwave attenuation at 36 GHz, *IEE Conf. Pub.* **98**, 45-51 (1973).

2. **Crane, R.K.**, Prediction of attenuation by rain, *IEEE Transactions on Communications*, **COM-28**, No. 9, 1717-1733 (1980).

3. **Ruthroff, C.L.**, Rain attenuation and radio path design, *The Bell System Technical Journal*, **49**, No. 1, 121-125, Jan. (1970).

4. **Weible, G.E.** and **Dressel, H.O.**, Propagation studies in millimeter wave link systems, *Proceedings of the IEEE*, **55**, No. 4, 497-512 (1967).

5. **Freeman, R.L.**, *Telecommunication Transmission Hanndbook*, Ch. 10, John Wiley & Sons (1981).

6. **Harden, B.N.**, **Norbury, J.R.** and **White, W.J.K.**, Measurements of rainfall for studies of millimetric radio attenuation, *Microwaves, Optics and Acoustics*, **1**, No. 6, 197-202 (1977).

7. **Harden, B.N.**, **Norbury, J.W.** and **White, W.J.K.**, Estimation of attenuation by rain on terrestrial radio links in the UK at frequencies from 10 to 100 GHz, *Microwaves, Optics and Acoustics*, **2**, No. 4, 79-104 (1978).

8. **Norbury, J.R.** and **White, W.J.K.**, Point rainfall rate measurements at Slough, U.K., *IEE Conf. Pub.* **98**, 190-196 (1973).

9. **Kumar, P.N.**, Precipitation fade statistics for 19/29-GHz COMSTAR Beacon Signals and 12-GHz radiometric measurements, *COMSAT Technical Review*, **12**, No. 1, 1-127, Spring (1982).

10. **Harman, L.K.,** Rain rate and atmospheric attenuation statistics at millimeter wave frequencies, *International Conf. on Communications, ICC* 74, *Conf. Record*, pp. 23B-1 to 23B-5, June 1974.

11. **Mogensen, G.** and **Stephansen, E.,** An estimation of methods for prediction of rain induced attenuation on L.O.S. paths, *Int. Conf. on Ant. and Prop., IEE Conf. Pub.* 169, 97-101, Nov. 1978.

12. **Sander, J.,** Rain attenuation of millimeter waves at $\lambda = 5.77$, 3.3, and 2 mm, *IEEE Trans. on Ant. and Prop.*, Vol. **AP-23,** No. 2, 213-230 (1975).

13. **Keizer, W.P.M.N., Snieder, J.** and **deHaan, C.D.,** Rain attenuation measurement at 94 GHz; comparison of theory and experiment, *AGARD Conf. Proc.* No. 254, 44-1/44-9 (1978).

14. **Gunn, R.** and **Kinzer, G.D.,** The terminal velocity of fall for water droplets in stagnant air, *J. Meteorol.*, **6,** 243-248 (1949).

15. **Oguchi, T.,** Scattering properties of Pruppacher and Pitter form rain drops and cross polarization due to rain: Calculation at 11, 13, 19.3 and 34.8 GHz, *Radio Science*, **12,** No. 1, 41-51, Jan-Feb. 1977.

16. **Hogg, D.C.,** and **Chu, T.,** The role of rain in satellite communications, *Proc. IEEE*, **63,** No. 9, 1308-1331, Sept. 1975.

17. **Brussaard, G.,** A meteorological model for rain-induced cross polarization, *IEEE Trans. on Ant. and Prop.*, **AP-24,** No. 1, 5-11 (1976).

18. **Evans, B.G.** and **Upton, S.A.J.,** Effect of rain drop shape on cross polarization/attenuation relationships, *Electronic Letters*, **17,** No. 1, 22-23, Jan. (1981).

19. **Pruppacher, H.R.** and **Pitter, R.L.,** A semi-empirical determination of the shape of cloud and rain drops, *J. Atmos. Sci.*, **28,** 86-94 (1971).

20. **Laws, J.O.** and **Parsons, D.A.,** The relation of rain-drop size to intensity, *Trans. Amer. Geophys. Union*, **24,** 453-460 (1943).

21. **Marshall, J.S.** and **Palmer, W.Mck.,** The distribution of rain drops with size, *J. Meterol.*, **5,** 165-166 (1948).

22. **Joss, J., Thams, J.C.** and **Waldvogel, A.,** The variation of rain drop size distribution at Locarno, *Proc. Intern. Conf. Cloud Physics*, Toronto, 369-373 (1968).

23. **Keizer, W.P.M.N., Snieder, J.** and **deHaan, C.D.,** Propagation measurements at 94 GHz and comparison of experimental rain attenuation with theoretical results derived from actually measured rain drop size distribution, *Intl. Conf. on Ant. and Prop., IEE Conf. Pub.* 169, 72-76, Nov. 1978.

24. **Furuhama, Y.,** Path-averaged raindrop size distributions from scattering measurements at 1.7, 11.5, 34.5 and 81.8 GHz, *IEEE Trans. on Ant. and Prop.*, **AP-29,** No. 2, 275-281 (1981).

25. **Bodtmann, W.F.** and **Ruthroff, C.L.,** Rain attenuation on short radio paths: Theory, experiment, and design, *The Bell System Technical Journal*, **53,** No.7, 1329-1348 (1974).

26. **Hata, M.** and **Doi, S.,** Propagation tests for 23 GHz and 40 GHz, *IEEE Journal on Selected Areas in Communications*, **SAC-1,** No. 4, 658-673, Sept. 1983.

27. **Norbury, J.R.** and **White, W.J.K.,** A rapid response rain gauge, *J. Phys. E.*, **4,** 601-602 (1971).

28. **Donnadian, G.,** Studies of the physical and radioelectric characteristics of rain with the aid of a photoelectric rain drop spectrometer, *J. Rech. Atmos.*, **VIII,** 253-266 (1974).

29. **Knollenberg, R. G.,** The optical array: an alternative to scattering or extinction for airborne particle size determination, *J. Appl. Meteorol.*, No. 9, 86-103 (1970).

30. **Joss, J., Cavalli, R.** and **Crane, R.K.,** Good agreement between theory and experiment for attenuation data, *J. Rech. Atmos.*, **8,** 299-318 (1974).

31. **Joss, J.,** Capabilities of measuring rainfall with radar over a river basin—experience with the Swiss radars, *Proc. Symp. Hydrolog. Research Basins, Sondeh. Landeohydrologie, Bern,* 143-152 (1982).

32. **Goldhirsch, J.,** and **Robinson, R.L.,** Attenuation and space diversity statistics calculated from radar reflectivity data of rain, *IEEE Trans. on Ant. and Prop.*, **AP-23,** No. 2, 221-227 (1975).

33. **Goldhirsh, J.,** Rain cell size statistics as a function of rain rate for attenuation modeling, *IEEE Trans. on Ant. and Prop.*, **AP-31,** No. 5, 799-801, Sept. 1983.

34. **Awaka, J., Nakamura, K.** and **Inomata, H.,** Bistatic rain-scatter experiment at 34.8 GHz, *IEEE Trans. on Ant. and Prop.*, **AP-31,** No. 5, 693-698, Sept. 1983.

35. **Fujita, M., Shinozuk, T., Ihara, T., Furuhama, Y.** and **Inoki, H.,** ETS-II experiments part IV: Characteristics of millimeter and centimeter wavelength propagation, *IEEE Transaction Aerospace & Electronics Systems,* **AES-16,** No. 5, 581-589, Sept. 1980.

36. **Hewitt, M.T.** and **Norbury, J.R.,** Correlation of fading on spaced microwave paths at 22 & 37 GHz, *IEE Pub.* 98, 250-255 (1973).

37. **Watson, P.A.,** Survey of measurements of attenuation by rain and other hydrometers, *Proc. IEE,* **123,** No. 9, 863-871 (1976).

38. **Wulpsberg, K.N.** and **Altshuler, E.E.,** Rain attenuation at 15 and 35 GHz, *IEEE Trans. on Ant. and Prop.*, **AP-20,** No. 2, 181-187 (1972).

39. **Zavody, A.M.,** Effect of scattering by rain on radiometer measurements at millimeter wavelengths, *Proc. IEE,* **121,** 4, 257-263 (1974).

40. **Guiraud, F.O., Howard, J.** and **Hogg, D.C.,** A dual-channel microwave radiometer for measurement of precipitable water vapor and liquid, *IEEE Trans. on geoscience electronics,* **GE-17,** No. 4, 129-136, Oct. 1979.

41. **Raina, M.K.** and **Uppal, G.S.,** Rain attenuation measurements over New Delhi with a microwave radiometer at 11 GHz, *IEEE Trans. on Ant. and Prop.*, **AP-29,** No. 6, 857-864, Nov. 1981.

42. **Davies, P.G.,** Radiometer studies of atmospheric attenuation of solar emission at 19 GHz, *Proc. IEE,* **118,** No. 6, 737-741, July 1971.

43. **Davies, P.G.,** Radiometer measurements of atmospheric attenuation at 19 and 37 GHz along sun-earth paths, *Proc. IEEE,* **120,** No. 2, 159-164, Feb. 1973.

44. **Davies, P.G.,** Slant path attenuation at frequencies above 10 GHz, *IEE Pub.* **98,** 141-149 (1973).

45. **Davies, P.G.** and **Croom, D.L.,** Diversity measurements of attenuation at 37 GHz with solar-tracking radiometers, *Electronic Letters,* **10,** No. 23, 482-483, Nov. 1974.

46. **Davies, P.G.,** Diversity measurements of attenuation at 37 GHz with sun-tracking radiometers in a 3-site network, *Proc. IEE,* **123,** No. 8, 765-769, Aug. 1976.

47. **Davies, P.G.** and **McKenzie, E.C.,** Review of slant path propagation measurements made at the applied laboratory, Slough, UK, *AGARD Conf. Proc.* No. 284, 9-1 to 9-22, Aug. 1980.

48. **Davies, P.G.** and **McKenzie, E.C.**, Review of SHF and EHF slant path propagation measurements made near Slough (UK), *IEE Proceedings*, **128**, Pt. H, No. 1, 53-65 (1981).

49. **Wilson, R.W.** and **Mammel, W.L.**, Results from a three radiometer path-diversity experiment, *IEE Pub.* **98**, 23-27 (1978).

50. **Horvath, E.**, Rain measurement equipment and measurement results, *Proc. Symp. Hydrology Research Basins, Sonderh Landeshydrologies Bern*, 133-141 (1982).

51. **Evans, B.G.** and **Throughton, J.**, Calculation of cross polarization due to precipitation, *IEE Conf. Pub.* **98**, 162-171 (1973).

قياس خواص الأمطار المتعلقة بانتشار الموجات الكهرومغنطيسية

* محمد عبد العزيز حسن ، ** عادل أحمد علي و ** محمد عبد الرحمن الحيدر
قسم الهندسة الكهربائية ، كلية الهندسة ، جامعة الملك سعود ، الرياض ، المملكة العربية السعودية .

يستعرض هذا البحث خواص الأمطار وطرق قياسها وذلك فيما يتعلق بتأثيرها على انتشار الموجات الكهرومغنطيسية ذات الطول المليمتري . ويبدأ البحث بدراسة معدل سقوط الأمطار وأهم الدراسات العملية التي أجريت لقياسه ، ثم يتعرض للخواص الأخرى كسرعة سقوط القطرات وشكلها وحجمها وزاوية ميلها أثناء السقوط كما يشتمل البحث على دراسة الطرق المباشرة وغير المباشرة لقياس الأمطار وأهم الأجهزة المستخدمة لذلك ، ويخلص الى مقارنة شاملة لطرق وأجهزة القياس موضحا مزايا وعيوب كل طريقة وذلك من خلال ستة قوائم مقارنة .

وينتهي البحث بذكر أهم المجالات التي تحتاج إلى المزيد من البحث والدراسة في هذا الصدد .

*أستاذ مساعد .
**أستاذ مشارك كلية الهندسة .